PETROGRAPHY AND GEOCHEMICAL CHARACTERIZATION OF THE LAMÉ ALKALIN BASALTS (SOUTHWESTERN MAYO KEBBI) IN THE CAMEROON CHAD VOLCANIC LINE: IMPLICATIONS FOR TECTONIC EVOLUTION AND MANTLE SOURCE

Abstract

The Lamé basalts, located in the Mayo Kebbi massif in southwestern Chad, display petrographic and geochemical features typical of intraplate alkaline magmas. Their homogeneous mineralogical composition (clinopyroxene, olivine, plagioclase, and iron oxides), combined with a relative enrichment in LREE compared to HREE, as well as V, Cr, Mg# contents and Nb/U ratios characteristic of OIB, indicate a HIMU-type mantle source with residual garnet. Variations in major and trace elements show that magmatic differentiation was dominated by fractional crystallization, with no evidence of crustal contamination. These geochemical signatures closely resemble those of alkaline magmas observed in the Tibesti, Ouaddaï and Lake Chad volcanic provinces, confirming their affiliation with the northern extension of the Cameroon Volcanic Line.

Keywords: Lamé, alkaline basalts, Cameroon–Chad Volcanic Line (CCVL), fractional crystallization, OIB and HIMU.

1. Introduction

The Cameroon Volcanic Line (CVL) represents a continental intraplate volcanic province in Central Africa (Figure 1a, b). This tectono-magmatic system, oriented along an azimuth of 030°, extends both over the oceanic crust in the Gulf of Guinea islands (Pagalu, São Tomé, Principe, and Bioko) and over the continental crust, from Mount Cameroon to the Lake Chad Basin [1]. Recent studies by [2] have highlighted the influence of mantle magmatism ranging from the Cretaceous–Paleocene to the Cenozoic, initially recognized in Cameroon and Chad, on either side of the positive gravity anomaly known as “Poli–Ounianga–Kebir.” This large-

scale magmatic province, oriented SW–NE, has been defined as the Cameroon–Chad Volcanic Line (CCVL).

In Chad, volcanic formations intrude Precambrian basement rocks as well as Mesozoic and Cenozoic sedimentary sequences [3,2]. They comprise both mafic rocks (eg. basalts, basanites) and felsic rocks (eg. trachytes, rhyolites, phonolite), reflecting significant magmatic diversity.

In this study, the petrographic and geochemical characteristics of the Lamé basalts, located in the Mayo Kebbi massif, are presented and compared with other basalts from Chad and Cameroon. The magmatic sources and tectonic evolution are discussed to provide new insights into the dynamics of this intraplate volcanic province.

2. Volcanic Geology of Chad

Chad is characterized by a Precambrian basement overlain by Mesozoic to Cenozoic sedimentary sequences deposited in the intracratonic basins of Iullemmeden and Chad, as well as in the Benue and Leré rift basins, where volcanic formations are also present (Figure 1b)[4,5,6,2]. Detailed studies have been carried out on volcanic formations in the Tibesti, Ouaddaï, and HadjerLamis regions.

The Tibesti Volcanic Province (TVP; Figure 1b) represents the main volcanic manifestation in Chad. It includes: (i) Miocene plateau volcanism, consisting of flood basalts and silicic lavas with intercalated ignimbritic deposits (17–8 Ma); (ii) basaltic scoria cones and associated lava flows (7–5 Ma); (iii) large Late Miocene central composite volcanoes aligned along a major NNE–SSW fault; (iv) extensive ignimbritic volcanoes (7–0.43 Ma); and (v) the TarsoTousside volcanic complex. These formations are located along the Tassilian flexure (NW–SE) and a major fault zone oriented NE–SW to NNE–SSW [7]. Geochemical data from [3] reveal, in the Emi Koussi region, a bimodal series composed of (1) a silica-saturated suite dominated by trachytes and a few trachyandesites, and (2) a silica-undersaturated suite

consisting of basalts and phonolites. Overall, available petrological and geochemical data indicate that volcanic activity is dominated by alkaline to peralkaline lavas, ranging from basanites to arfvedsonite ± acmite-bearing rhyolites, derived from fractional crystallization of alkaline magmas probably originating from a metasomatized mantle source [8,3].

In the northern part of the Ouaddaï massif, theralites and basalts crop out [9]. Recent work by [2] shows that these volcanic rocks represent a continuation of those of the Cameroon Volcanic Line (CVL), located further to the southeast within the Central African Rift System. These basanites correspond to OIB-type basalts (Ocean Island Basalts), produced by fractional crystallization without any evidence of crustal contamination. The parental magmas are therefore derived from partial melting of a metasomatized subcontinental lithospheric root, reactivated during the formation of the Cenozoic Central African Rift System.

In the HadjerLamis region (Lake Chad), volcanic rocks are dated to the Cretaceous–Paleocene transition and consist mainly of peralkaline rhyolites formed by fractional crystallization of alkaline parental magmas derived from a metasomatized mantle source [10,11]. Based on geochronological and isotopic data, [11] associate these silicic rocks with Late Cretaceous extensional volcanism in the Termit Basin, controlled by the reactivation of Pan-African suture zones during the opening of the central Atlantic Ocean.

In the Mayo Kebbi region, volcanic formations are poorly represented (Figure 1c). They consist mainly of metabasalts and basalts corresponding to E-MORB [12] and OIB [13].

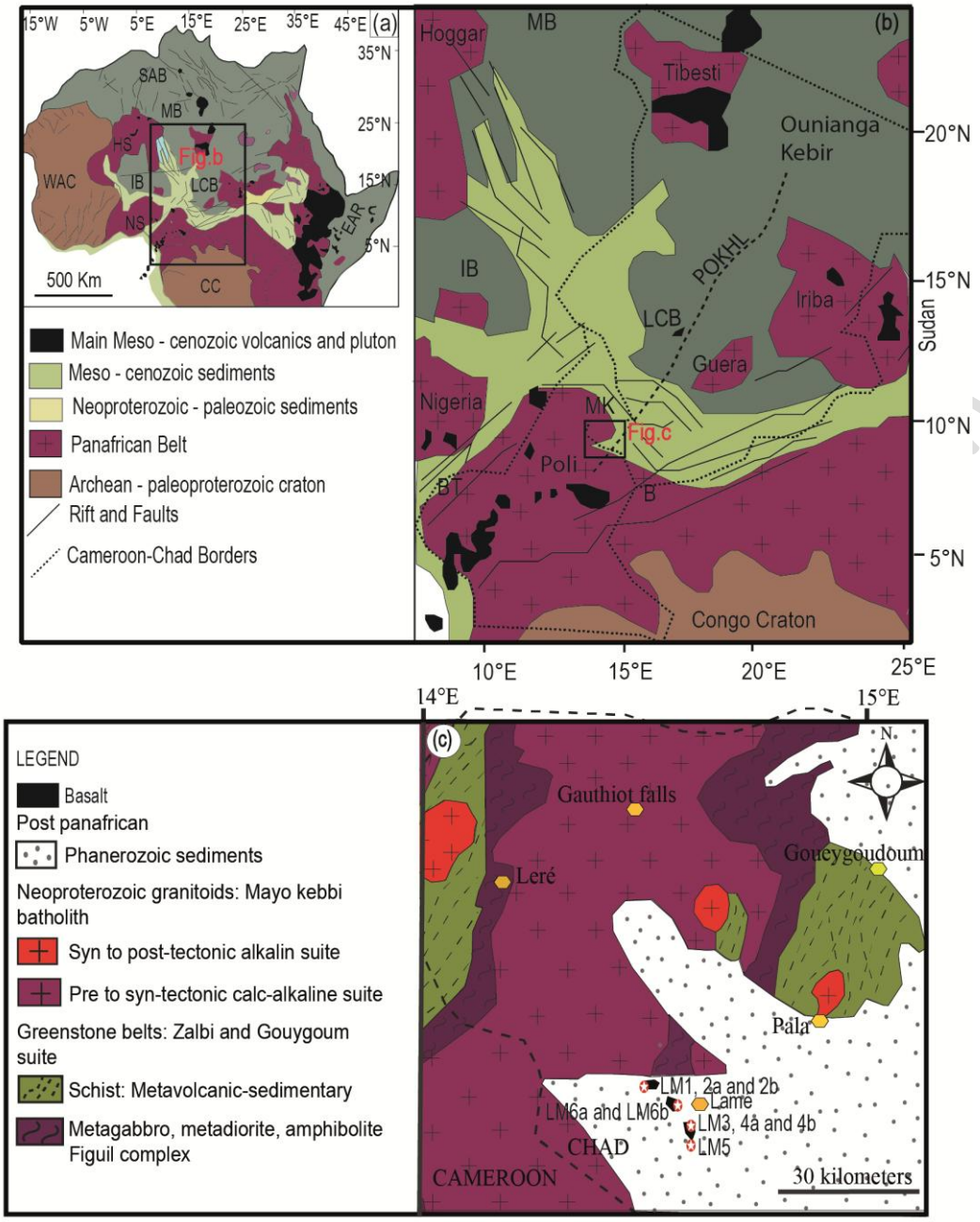

Figure 1.(a) Tectonic Map of Africa: Location map of the Cameroon Volcanic Line (CVL). The main geologic features of Africa are indicated. (b) Structural map of Central Africa Rift System [14,6]showing the Cameroon Volcanic Line (CVL) and its extension in chad. The names of the main Early Cretaceous intracontinental rifts are indicated. SAB = Sud Algerian Basin; MB =Murzuk Basin; IB = Iullemeden Basin; LCB = Lake Chad Basin; BT = Benue Trough; MK = Mayo Kebbi; B = Baibokoum; WAC = West African Craton; CC = Congo Craton; HN = Hoggar Shield; NS = Nigerian Shield; EAR = East African Rift; POKH = Poli–

Ounianga–Kebir heavy [15. (c) Geological sketch map of the Mayo Kebbi and neighbouring regions. The study area with the position of the samples to be used in the geochemical study.

3. Analytical methods

Geological field campaigns were conducted in Lamé locality in the southwest of Chad. This phase enabled the macroscopic identification of rock facies and the collection of key lithological parameters, including color, texture, mineralogical composition and degree of alteration. A total of nine (09) fresh, unaltered samples were selected.

Rocks samples were sawed into chips for thin section preparation and trimmed to small blocks for geochemical investigations. About 200 to 500 g of each sample was crushed into a steel jaw crusher and then pulverized with an agate ball mill. Powders were digested using an alkali fusion procedure where the powder was mixed to lithium metaborate and melted to produce a glass pellet. The pellet was digested into diluted nitric acid before analyses. Analyses and digestions were made at the ALS Geochemistry-Loughrea (Irland). Prepared samples (0.100 g) are added to lithium metaborate/lithium tetraborate flux, mixed well and fused in a furnace at 1000°C. The resulting melt is then cooled and dissolved in 100 mL of 4% nitric acid/2% hydrochloric acid. This solution is then analysed by ICP-AES and the results are corrected for spectral inter-element interferences. Oxide concentration is calculated from the determined elemental concentration and the result is reported in that format. The Whole Rock analysis is determined in conjunction with a loss-on-ignition at 1000°C. The resulting data from both determinations are combined to produce a “total”. For the determination of trace-elements, the samples were mixed well and fused in a furnace at 1025°C. The resulting melt is then cooled and dissolved in an acid mixture containing nitric, hydrochloric and hydrofluoric acids. This solution isthenanalyzed by ICP–MS.

4. Petrographic Description

The basalts from the Lamé quarry (Figure 2a, b), located in the Mayo Kebbi massif in southwestern Chad, occur as rounded blocks with a gray to yellowish weathered surface and a dark fracture, where minerals such as plagioclase can be distinguished. Their massive and dark appearance reflects a high proportion of ferromagnesian minerals (Figure 2d, e).

Thin-section petrographic analysis reveals a microlitic porphyritic texture (Figure 2c, f), dominated by clinopyroxene (40–50%), olivine (30–40%), plagioclase (5–10%), and opaque minerals (< 5%). Clinopyroxene occurs in two generations: a fine-grained matrix, often altered, and automorphic to xenomorphic phenocrysts, elongated and marked by distinct cleavage. Olivine crystals, sometimes zoned, appear as lozenge-shaped phenocrysts with occasional well-developed cleavage. Plagioclase is scarce and frequently altered, with some crystals showing a dusty or mottled grayish appearance due to the development of finely crystallized alteration products. Opaque mineralsoccur as inclusions withinclinopyroxene and olivine crystals

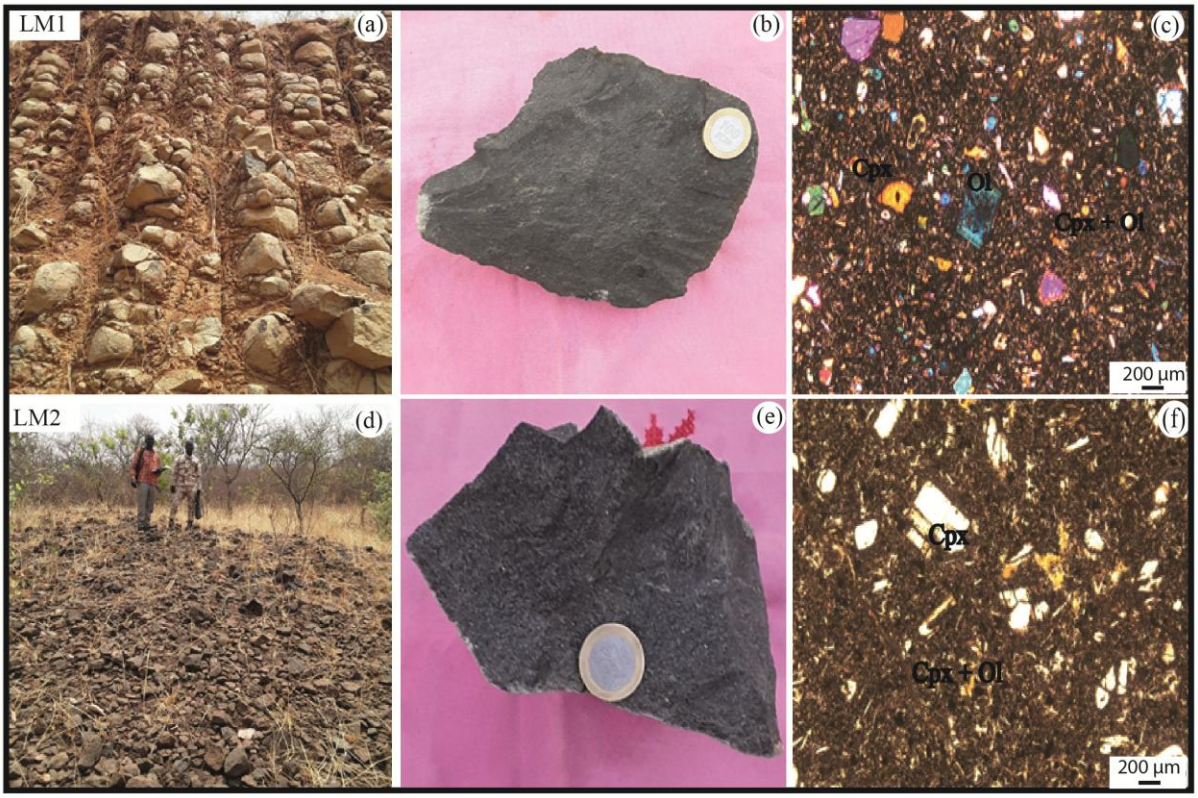

Figure 2: Macroscopic and microscopic photographs of Lamé basalt. (a) and (b) Outcrop and hand specimen showing rounded basalt blocks in a trench. (c) Microlitic porphyritic texture of Lamé basalt. (d) and (e) Outcrop and specimen of dark-colored basalt, displaying a microlitic porphyritic texture. (f) Microscopic view highlighting the same texture.

5. Geochemistry

The chemical compositions of nine (09) representative basalt samples from Lamé are reported in Table 1. Unlike the basalts from Emi Koussi and Iriba, which plot between basanites and tephrites in the SiO_2 vs $Na_2O + K_2O$ diagram (Figure 3a), the Lamé samples are distributed between basanites and basalts.

In the Nb/Y vs Zr/Ti diagram (Figure 3b), all of these rocks correspond to alkaline basalts. This classification indicates that, in most of the samples, the concentrations of mobile elements (Na and K) as well as immobile elements (Nb, Y, Zr, Ti) have not been significantly modified by subsequent metasomatic processes.

These results suggest that the Lamé basalts retain their primary geochemical signatures, representative of intraplate alkaline magmatism, and can be reliably compared with other volcanic provinces along the Cameroon–Chad Volcanic Line (CCVL).

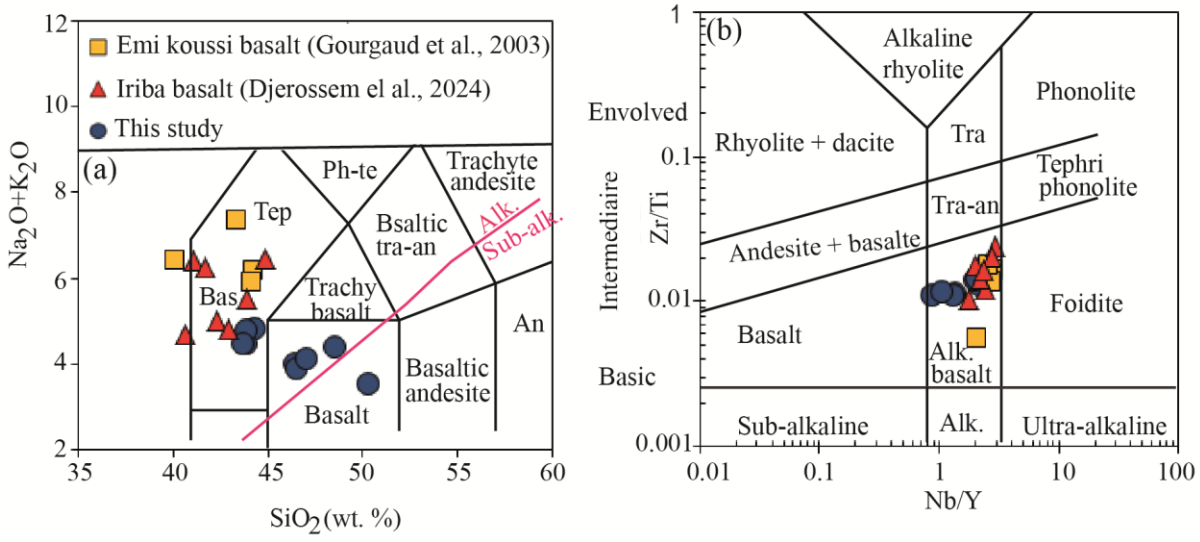

Figure 3. Total alkali-silica diagram [16].The red line separates the alkaline and the subalkaline domain, according to [17]. (b) Zr/Ti vs. Nb/Yb diagram [17]. Bas= basanite, Tep= tephrite, Ph-te= phonolite-tephrite, tra-an= trachy-andesite, An= andesite, Tra= trachyte, Alk.= alkaline.

5.1. Major Element Compositions

All analyzed basalts are characterized by SiO_2 contents ranging from 43.7 to 50.3 wt.%. Their alkali contents are relatively low ($3.52 \leq Na_2O + K_2O \leq 4.77$) compared to those observed in the Emi Koussi basalts ($5.93 \leq Na_2O + K_2O \leq 7.4$) and the Iriba basalts ($4.69 \leq Na_2O + K_2O \leq 6.43$). The Lamé basalts display relatively high MgO values ($7.42 \leq MgO \leq 9.33$) with Mg# values ranging from 55.23 to 59.10. Fe_2O_3 contents (12–13.75 wt.%) and Al_2O_3 contents (13.01–13.75 wt.%) are nearly identical, while TiO_2 values vary between 1.68 and 2.72 wt.%. In binary Arker-type diagrams (oxide vs. SiO_2, Figure 4), all samples show negative correlations with Fe_2O_3, CaO, MgO, K_2O, TiO_2, MnO, and P_2O_5. Al_2O_3 increases with SiO_2 content, indicating the absence of plagioclase fractionation. The decrease in Fe_2O_3, MgO, TiO_2, MnO, and P_2O_5 with increasing SiO_2 is related to the crystallization of olivine, clinopyroxene, Fe–Ti oxides, and apatite.

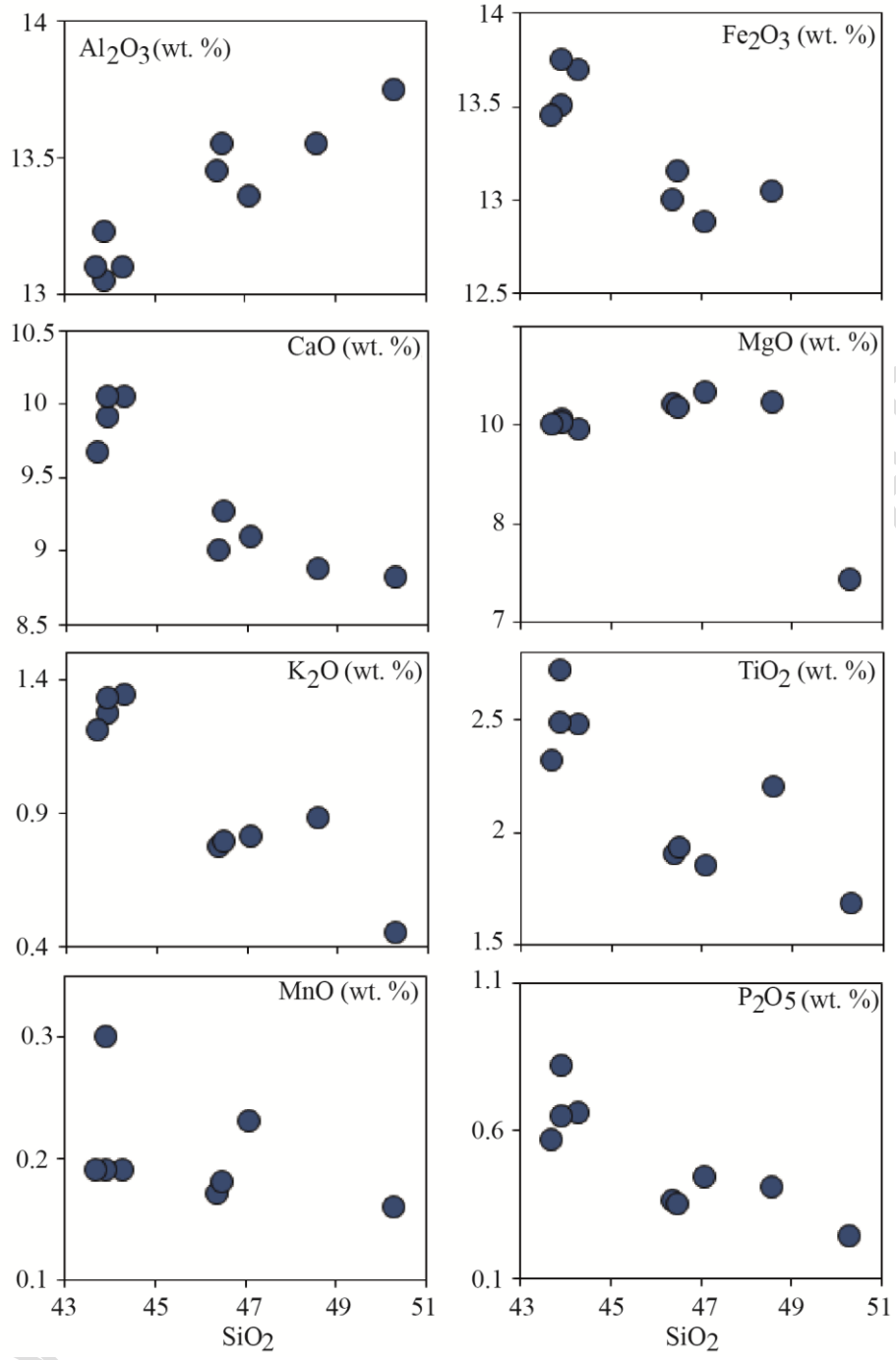

Figure 4. Major elements (wt%) versus SiO_2 distribution of Lamé basalts

5.2. Trace Element Compositions

The Lamé basalts are characterized by Cr and V contents ranging from 234 to 330 ppm and 187 to 235 ppm, respectively. Concentrations of large-ion lithophile elements (LILEs) such as Ba and Sr vary between 161–420 ppm and 144–1015 ppm. In trace element variation

diagrams including Zr, La, V, Sr, Rb, Ba, and Nb, positive linear correlations are observed with increasing Th content (Figure 5). Cr concentrations decrease as Th increases.

In chondrite-normalized rare earth element (REE) diagrams (McDonough et al., 1989; Figure 6a), the Lamé basalts display slight enrichment in light REEs ($5.25 \leq (La/Gd)N \leq 15.54$) relative to middle REEs (MREE) and heavy REEs ($2.43 \leq (La/Gd)N \leq 4.16$). Their REE patterns are broadly parallel to those of Ocean Island Basalts (OIB). A weak positive Eu anomaly is also observed ($1.01 \leq (Eu/Eu^*) \leq 1.10$).

In primitive mantle-normalized diagrams (Figure 6b), the Lamé basalts show slight positive anomalies in Ba, Nb-Ta, and Sr, while negative anomalies are observed in Th-U-K and Pr. Overall, their geochemical profiles closely resemble those of OIB, in contrast to N-MORB and E-MORB.

Table 1. Whole rock composition of Lamé basalts

Sample	LM1	LM2a	LM2b	LM3	LM4a	LM4b	LM5	LM6a	LM6b
SiO_2	50.30	44.30	43.90	43.90	43.70	48.60	46.40	46.50	47.10
Al_2O_3	13.75	13.10	13.23	13.05	13.10	13.55	13.45	13.55	13.36
Fe_2O_3	12.00	13.70	13.51	13.75	13.45	13.05	13.00	13.15	12.88
CaO	8.82	10.05	9.91	10.05	9.67	8.88	9.00	9.27	9.09
MgO	7.42	8.96	9.05	9.02	9.01	9.23	9.22	9.17	9.33
Na_2O	3.07	3.48	3.21	3.44	3.27	3.50	3.24	3.10	3.30
K_2O	0.45	1.34	1.27	1.33	1.21	0.88	0.77	0.79	0.81
Cr_2O_3	0.04	0.03	0.05	0.03	0.03	0.05	0.04	0.04	0.03
TiO_2	1.68	2.48	2.72	2.49	2.32	2.20	1.90	1.93	1.85
MnO	0.16	0.19	0.30	0.19	0.19	1.15	0.17	0.18	0.23
P_2O_5	0.24	0.66	0.82	0.65	0.57	0.41	0.36	0.35	0.44
SrO	0.04	0.10	0.22	0.11	0.12	0.05	0.07	0.08	0.06
BaO	0.02	0.05	0.07	0.04	0.05	0.02	0.03	0.02	0.02
LOI	0.69	0.83	0.77	0.94	0.91	1.08	1.03	0.81	0.90
Total	98.68	99.27	99.03	98.99	97.60	102.65	98.68	98.94	99.40
Na_2O+K_2O	3.52	4.82	4.48	4.77	4.48	4.38	4.01	3.89	4.11
Mg#	55.23	56.61	57.20	56.68	57.20	58.52	58.59	58.18	59.10
Sc	21.40	19.50	20.04	20.20	20.80	19.50	21.60	21.90	20.60
V	187.00	232.00	191.00	235.00	233.00	224.00	215.00	207.00	213.00
Cr	330.00	234.00	319.00	239.00	254.00	243.00	323.00	304.00	298.00
Rb	11.10	27.20	26.50	27.50	25.60	25.10	16.80	17.20	16.65
Sr	344.00	869.00	850.00	899.00	1015.00	1011.00	573.00	582.00	577.00
Zr	110.00	216.00	210.00	219.00	192.00	189.00	129.00	126.00	130.00

Nb	17.15	51.80	49.00	53.60	46.40	47.10	27.40	26.50	25.40
Cs	0.13	0.36	0.26	0.35	0.35	0.35	0.46	0.33	0.29
Ba	161.00	391.00	387.00	394.00	418.00	420.00	247.00	211.00	215.00
Y	19.80	23.50	22.00	23.70	23.00	23.00	19.70	20.00	24.00
La	10.70	32.50	30.30	32.60	27.90	25.90	16.20	15.90	14.10
Ce	22.50	66.70	58.92	67.30	57.80	56.90	34.00	33.80	32.70
Pr	2.82	7.74	7.49	7.97	6.93	7.10	4.09	4.17	5.20
Nd	13.30	33.10	32.90	33.40	29.20	31.20	18.30	18.20	19.50
Sm	3.61	7.32	6.88	7.30	6.52	7.30	4.53	4.49	4.37
Eu	1.34	2.47	2.51	2.44	2.23	2.41	1.60	1.61	1.54
Gd	4.55	6.98	7.20	7.24	6.68	6.82	4.96	4.76	4.12
Tb	0.68	0.96	0.87	0.96	0.90	0.94	0.73	0.70	0.80
Dy	3.97	5.16	5.23	5.38	4.77	4.54	4.15	4.00	5.16
Ho	0.73	0.90	0.80	0.91	0.86	0.90	0.72	0.72	0.80
Er	1.99	2.24	2.56	2.19	2.08	2.15	1.96	1.86	1.78
Tm	0.25	0.27	0.30	0.25	0.27	0.17	0.23	0.23	0.31
Yb	1.46	1.50	1.43	1.58	1.65	1.55	1.42	1.46	1.40
Lu	0.22	0.21	0.20	0.20	0.24	0.30	0.19	0.19	0.20
Hf	3.00	4.77	4.11	4.65	4.26	4.23	3.09	2.99	3.00
Ta	1.00	2.80	2.50	2.90	2.30	2.10	1.40	1.40	1.70
W	1.00	0.90	0.80	0.90	1.10	1.60	0.90	0.70	0.80
Th	1.23	3.71	3.12	3.64	3.16	3.21	1.78	1.70	1.54
U	0.32	1.02	1.05	0.99	0.89	0.90	0.51	0.47	0.51

168

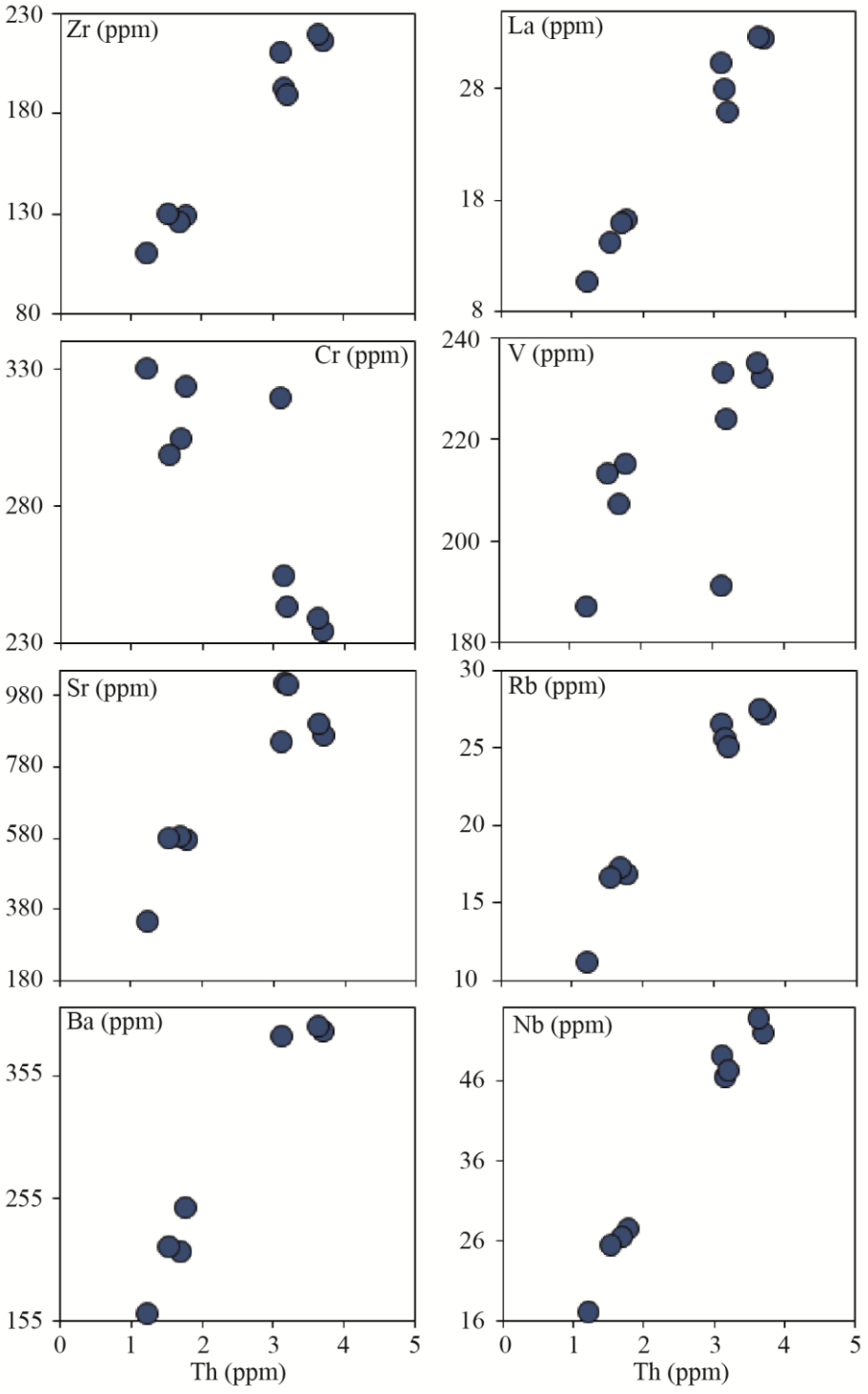

169

170 Figure 5: Trace elements distribution of Lamé basalts.

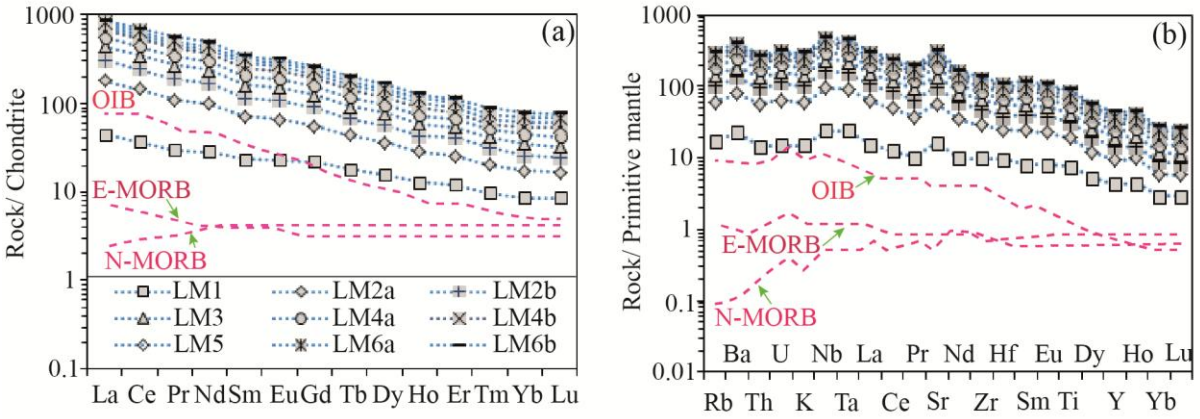

Figure 6.(a) Chondrite normalized REE paterns and (b) primitive mantle normalized trace elements diagrams of Lamé basalts. The normalization values are after [18].

6. Discussion

6.1. Fractional Crystallization and Crustal Contamination of the Lamé Basalt

Monogenetic volcanic edifices are typically characterized by eruptions fed by relatively primitive basaltic magmas, which undergo limited fractional crystallization and may occasionally exhibit signatures of crustal contamination [19,20,21,22]. This pattern is also observed in the Lamé basalts, which display decreasing concentrations of oxides such as Fe_2O_3, MgO, TiO_2, MnO, and P_2O_5 with increasing SiO_2 content (Figure 5). These trends reflect fractional crystallization of olivine, clinopyroxene, Fe–Ti oxides, and apatite. In the Ba vs. Sr diagram (Figure 7a), the Lamé basalts show dominant fractionation of olivine and clinopyroxene, comparable to the Iriba basalts [2]. Such features are typical of magmas emplaced through fractional crystallization processes. This is further supported by the Rb vs. Sr diagram (Figure 7b), where Sr values remain relatively constant despite increasing Rb concentrations. Fractional crystallization is also indicated by Mg# values (55.23–59.10), which are lower than those of primary magmas (Mg# = 68–72) [23,24,25,26].

In small-volume volcanoes, magmas ascend rapidly through simple conduits, but interaction with crustal rocks remains possible [27]. Along the Cameroon Volcanic Line (CVL), crustal

contamination is well documented for mafic and felsic lavas of large volcanic edifices [26,28,29]. However, studies of monogenetic volcanoes in the southern CVL have not revealed significant crustal contamination [30,31]. Investigations in the CVL extension into Chad, including Tibesti [5] and Ouaddaï [2], similarly show no evidence of crustal contamination in basalts.

Negative Th and U anomalies observed in the Lamé basalts could suggest crustal contamination. [26]demonstrated that the most primitive lavas (MgO ≈ 6 wt.%) exhibit La/Nb ratios below 0.8. As MgO decreases through fractional crystallization, La/Nb and $^{87}Sr/^{86}Sr$ ratios increase, reflecting contamination by a component enriched in La/Nb and $^{87}Sr/^{86}Sr$, typical of the upper continental crust. Despite the absence of isotopic data, the Lamé basalts are characterized by MgO contents (7.42–9.33 wt.%) slightly higher than 6 wt.% and La/Nb ratios (0.54–0.63) below 0.8. These values confirm that crustal contamination did not affect the Lamé basalts.

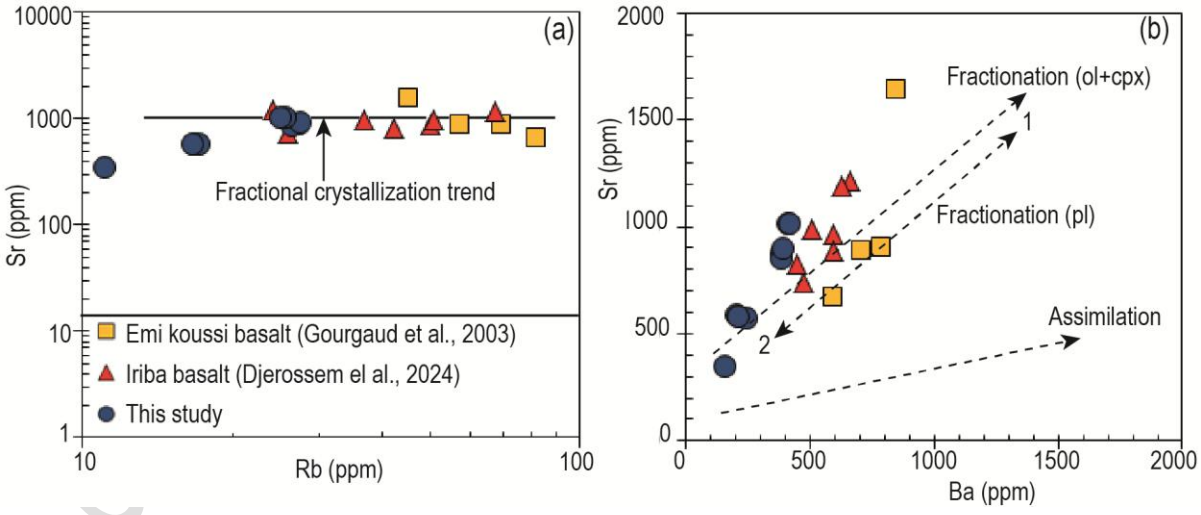

Figure 7.(a) Illustration of fractional crystallization trend in Rb versus Sr diagram [32] and (b) illustration of olivine and clinopyroxene fractionation in the Sr versus Ba diagramof [33].

6.2. Mantle Source of the Lamé Basalts and Conditions of Partial Melting

The Lamé basalts are distinguished by V contents (187–235 ppm), Cr contents (234–330 ppm), Mg# values of 55–58.6, and Nb/U ratios of 50–56.4. These values are consistent with a mantle origin and comparable to reference compositions (V ≈ 151 ppm; Cr ≈ 151 ppm; Mg# ≈ 60; Nb/U ≈ 30) [34,35]. The Th/Yb–Nb/Yb diagram (Figure 8a) confirms partial melting of the mantle without evidence of subduction-related signatures or crustal contamination. The TiO_2/Yb vs. Nb/Yb and V vs. Ti relationships (Figure 8b, c) indicate an alkaline affinity, typical of OIB close to HIMU sources. These features are analogous to those of basalts from Tibesti and Ouaddaï [3,2] as well as those from Cameroon [36,37].

Diagrams in Figure 8d, e, f reveal the presence of garnet (4–8%) in the source, corroborated by (Tb/Yb)N ratios (2.11–2.91), which exceed the threshold of 1.7 [38]. The degree of partial melting is estimated between 3 and 8%, comparable to that of the Mbengwi basanites (5–8%)[39], the Ouaddaï basalts (2–4% and 8%)[2], and the Emi Koussi basalts (1–4%) [3].

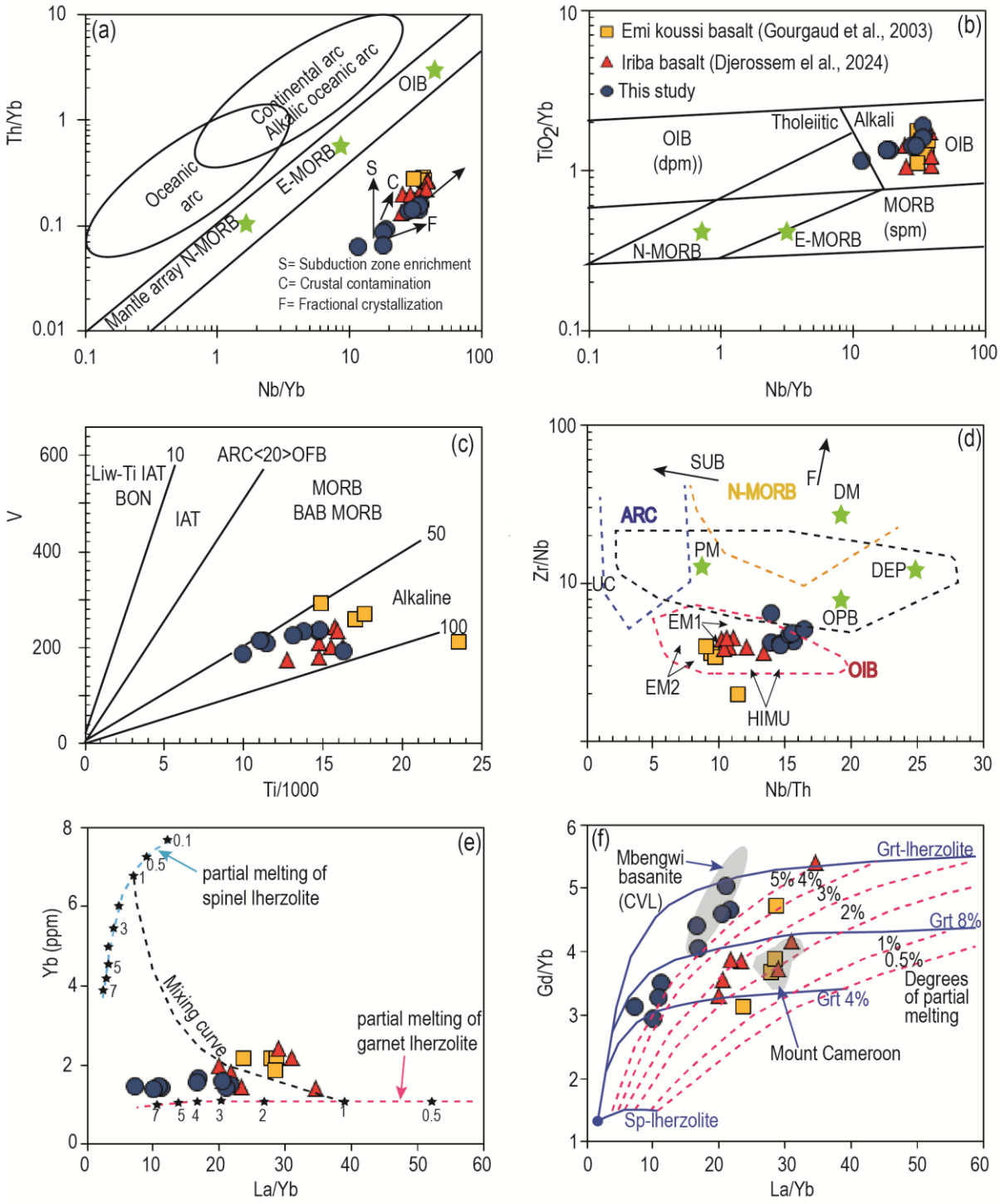

219

220 Figure 8. Diagramme de discrimination montrant les composantes de composition
221 mantellique et les champs de basaltes d'environnements géodynamiques variés. (a) Th/Yb-
222 Nb/Yb, (b) TiO2/Yb-Nb/Yb[40], (c) Ti-V [41] et (d) Zr/Nb-Nb/Th[42]. Les flèches en (d)
223 indique l'effet de la fusion partielle en équilibre (F) et de la subduction (SUB). (e) Plots of
224 Yb vs. La/Yb from [43]. The numbers of the curves denote degree of melting in percent,

using the partition coefficients of [44]. (f) Gd/Yb versus La/Yb diagram [45] illustrating the partial melting of Lamé basalts. The curves at Grt 4% and 8% correspond to the garnet content in the source [Halliday et al., 1995]. CVL=CameroonVolcanic Line. UC= croute continentale supérieure; PM= manteau primitif; DM= manteau supérieur appauvri; HIMU= source haut U/Pb; EM1 and EM2= sources de manteau enrichies; ARC= basalte d'arc; N-MORB= basalte de ride médio-océanique normale; OIB= basalte d'île océanique; DEP= manteau profond appauvri; EN= composante enrichie; REC= composante recyclée.

7. Conclusion

This study presents petrographic and geochemical data on the Lamé basalts, located in the Mayo Kebbi massif in southwestern Chad. These basalts display an alkaline affinity and were produced through fractional crystallization, with major crystallization of clinopyroxene and olivine, followed by plagioclase and opaque minerals. They show no evidence of crustal contamination and correspond to OIB-type magmas generated by partial melting at rates of 3–8%. Their mantle source is characterized as HIMU, containing 4–8% residual garnet.

The Lamé basalts share geochemical and petrographic similarities with alkaline magmas observed in Tibesti, Ouaddaï and Lake Chad, which are considered part of the northern extension of the Cameroon Volcanic Line. The study of the Lamé basalts thus strengthens the hypothesis of a large magmatic province, the Cameroon–Chad Volcanic Line (CCVL), controlled by the dynamics of the Central African Rift System and the reactivation of a metasomatized subcontinental lithospheric mantle.

Acknowledgement

This study was conducted as part of the research activities led by the first author. We extend our sincere gratitude to the administrative authorities of Lamé for their valuable collaboration and for authorizing the field campaigns. We thank the team at ALS Geochemistry-

Loughrea(Ireland) for their professionalism and commitment, which enabled the completion of geochemical analyses.

Reference

1. Wandji, P., Tchokona, S.D., Bardintzeff, J.M., Bellon, H., &Platevoet, B. (2008). Rhyolites of the Mbépit Massif in the Cameroon Volcanic Line: an early extrusive volcanic episode of Eocene age. *Mineralogy and Petrology*, 94, 271-286

2. Djerossem, F.N., Mbassa, B.J., Vanderhaeghe, O. and Gregoire, M. (2024). The Iriba Alkaline Basalts, an Expression of Mantle-Derived Cretaceous Magmatism of the Cameroon-Chad Volcanic Line along the Central Africa Rift System. *ComptesRendus. Geoscience*, 356, 231-248.

3. Gourgaud, A., & Vincent, P. M. (2003). Petrology of two continental alkaline intraplate series at Emi Koussi volcano, Tibesti, Chad. *Journal of Volcanology and Geothermal Research*, 129, 261–290.

4. Bessoles, B., & Trompette, R. (1980). La chaine panafricaine. Zone mobile d'Afrique Centrale (partie sud) et zone soudanaise, volume 92 of Mémoire du Bureau de Recherches Geologiques et Minieres.Editions B.R.G.M., Orleans.

5. Guiraud, R., &Maurin, J-C. (1992). Early Cretaceous rifts of Western and Central Africa: an overview. *Tectonophysics*, 213, 153–168.

6. Milesi, J.P., Frizonde Lamotte, D., De Kock, G., &Toteu, F. (2010). In CGMW and UNESCO, editors, *Tectonic Map of Africa (2nd edited), scale 1:10,000,000*. CCGM-CCGM, Paris.

7. Deniel, C., Vincent, P.M., Beauvilain, V., &Gourgaud, A. (2015). The Cenozoic volcanic province of Tibesti (Sahara of Chad): major units, chronology, and structural features. *Bulletin of Volcanology*, 77, 74.

8. Vicat, J.P, Pouclet, A., Bellion, Y., Doumnang, J.C. (2002). Les rhyolites hyperalcalines (pantellérites) du lac Tchad. Composition et signification tectonomagmatique. C R Geosciences 334:885–891.

9. Gsell, J. and Sonnet, J. (1962). Prospection de reconnaissance sur la coupure de Niere (feuille de Niere N° ND 34 NE 0.80-E.8). *Institut Equatorial de Recherches et d'Etudes Geologiques et Minieres.*

10. Mbowou, G.I.B., Lagmet, C., Nomade, S., Ngounouno, I., Bernard Deruelle, B., and Ohnenstetter, D. (2012). Petrology of the late cretaceous peralkaline rhyolites (pantellerite and comendite) from Lake Chad, Central Africa. *Journal of Geosciences*, 57, 127–141.

11. Shellnutt, J.G., Lee, T.Y., Torng, P.K., Yang, C.C., and Lee, Y.H. (2016). Late Cretaceous intraplate silicic volcanic rocks from the Lake Chad region: An extension of the Cameroon volcanic line? *Geochem. Geophys. Geosyst.*, 17, 2803–2824.

12. Doumnang, J.C. (2006).Geologie des formations Neoproterozoiques du Mayo-Kebbi (Sud-Ouest du Tchad), Apports de la petrologie et de la geochimie, implications sur la geodynamique au Pan-Africain. *Master'sThesis, Universite d'Orleans (France)*.

13. Isseini, M. (2011). Croissance et differenciation crustales au Neoproterozoique: Exemple du domaine panafricain du Mayo-Kebbi au Sud-Ouest du Tchad. *Master'sThesis, Universite Henri Poincare*.

14. Kogbe, C.A. (1981). Cretaceous and tertiary of the Iullemmeden basin inNigeria (West Africa). *Cretac. Res.*, 2, 129–186.

15. Louis, P. (1970). Contribution geophysique a la connaissance geologique du bassin du lac Tchad, volume42 of Bulletin de l'Office de la Recherche Scientifique et Technique Outre-Mer. *ORSTOM, Paris*.

16. Le Bas, M. J., Le Maitre, R.W., Streckeisen, A., and Zanettin, B. (1986). A chemical classification of volcanic rocks based on the total alkali-silica diagram. *Journal of Petrology*, 27, 745–750.

17. Irvine, T.N. and Baragar, W.R.A. (1971). A guide to the chemical classification of the common rocks. *Canada Journal of Earth Sciences*, 8, 523–548.

18. Sun, S.S. and Mcdonough, W. F. (1989). Chemical and isotopic systematic of oceanic basalts: implications of mantle composition and processes. In Saunders, A. .andNorry, M. ., editors, *Magmatismin Ocean Basins*, volume 42 of *Geological Society,London, Special Publications, 42*, pages 313–345. Geological Society of London.

19. Nkouathio, D.G., KagouDongmo, A., Bardintzeff, J.M., Wandji, P., Bellon, H., and Pouclet, A. (2008). Evolution of volcanism in graben and horst structures along the Cenozoic Cameroon Line (Africa): implications for tectonic evolution and mantle source composition. *Mineralogy and Petrology*, 94, 287-303.

20. Smith, I.E.M., Blake, S., Wilson, C.J.N., and Houghton, B.F. (2008). Deep-seated fractionation during the rise of a small-volume basalt magma batch: Crater Hill, Auckland, New Zealand. *Contrib Miner Petrol*, 155(4):511–527

21. Németh, K., White, J.D.L., Reay, A., and Martin, U. (2003). Compositional variation during monogenetic volcano growth and its implications for magma supply to continental volcanic fields. *J GeolSoLond* 160, 523–530.

22. Schmitt, F.H.,Schmitt, A.K.,Gerdes, A., and Harvey, J.C. (2021). Magma accumulation underneath Laacher See volcano from detrital zircon in modern streams. *Journal of the geological society*, 180 (1).

23. Frey, F.A., Green, D.H., and Roy, S.D. (1978). Integrated models of basalts petrogenesis: a study of quartz tholeiites to olivine melilites from South Eastern Australia utilizing geochemical and experimental petrological data. *J. Pet.*, 19, 463–513.

24. Tatsumi, O., Sakuyama, M.,Fukuyama, H.,&Kushiro,I. (1998). Generation of arc basalt magmas and thermal structure of the mantle wedge in subduction zones. *Journal of geophysical research*, 88, 5815-5825

25. Jung, S. and Masberg, P. (1998). Major and trace element systematics and isotope geochemistry of Cenozoic mafic volcanic rocks from the Vogelsberg (central Germany): Constraints on the origin of continental alkaline and tholeiitic basalts and their mantle sources. *Journal of Volcanology and Geothermal Research*, 86, 151–177.

26. Kamgang, P., Chazot, G., Njonfang, E., TchuimegnieNgongang, N.B., &Tchoua, M.F. (2013). Mantle sources and magma evolution beneath the Cameroon Volcanic Line: Geochemistry of mafic rocks from the Bamenda Mountains (NW Cameroon). *Gondwana Res* 24(2):727–741.

27. Smith, I.E.M.,&Németh, K. (2017). Source to surface model of mono-genetic volcanism: a critical review. In: Németh K, Carrasco-Nunez G, Aranda-Gomez JJ, Smith IEM (eds) Monogenetic volcanism. *The Geological Society Publishing House, Bath, UK, Special Publications*, 446.

28. Wotchoko, P., Nkouathio, D.G., KouankapNono, G.D., Chenyi, M.L.V., Guedjeo, C.S., Bulam, A.T., TchokonaSeuwui, D., &Seplong, Y. (2017).Petrogenesis of Lava from Wainama West, Mount Oku (CVL): source characterization and magma evolution. *J GeosciGeomat*, 5, 1–11.

29. Bate Tibang, E.E., Suh, C.E., Cottle, J., Ateh, I.K, Tiabou, F.A., Nche, A.L., Che, V.B., &Vishiti, A. (2017). Petrology and Geochronology of felsic volcanics in the Sabga area (Bamenda Highlands): implications for age variation along the Cameroon Volcanic Line. *J Geosci*, 62, 231–246.

30. Nkouathio, D.G., Ménard, J.J., Wandji, P., &Bardintzeff, J.M. (2002). The Tombel graben (West Cameroon): a recent monogenetic volcanic field of the Cameroon Line. *J Afr Earth Sci*, 35, 285–300.

31. Tamen, J., Nkoumbou, C., Mouafo, L., Reusser, E., Tchoua, M.F. (2007).Petrology and geochemistry of monogenetic volcanoes of the Barombi Koto volcanic field (Kumba graben, Cameroon volcanic line): Implications for mantle source characteristics. *C R Geosci* 339:799–809.

32. Xu, C., Huang, Z., Qi, L., Fu, P., Liu, C., Li, E., and Gung, T. (2007). Geochemistry of Cretaceous granites from Mianning in the Panix region, Sichuan Province, southwestern China: implications for their generation. *J. Asian. Earth Sci.*, 29, 737–750.

33. Franz, G., Steiner, G., Volker, F., Pudlo, D., and Hammerschmidt, K. (1999). Plume related alkaline magmatism in central Africa theMeidob Hills (W Sudan). *Chem. Geol.*, 157, 27–47.

34. Hofmann, C., Courtillot, V., Feraud, G., Rochette, P., Yirgu, G., Ketefo, E. (1997) Timing of the Ethiopian Flood Basalt Event and Implications for Plume Birth and Global Change. *Nature*, 389, 838-841.

35. Moyen, F., Laurent, O., Chelle-Michou, C., Couzinie, S., Vanderhaeghe, O., Zeh, A. (2017).Collision Vs. Subduction-Related Magmatism: Two Contrasting Ways of Granite Formation and Implications for Crustal Growth. *Lithos* , 277, 154-177.

36. Ngounouno, I., Deruelle, B., and Demaiffe, D. (2000). Petrology of the bimodal Cenozoic volcanism of the Kapsiki plateau (northernmost Cameroon, Central Africa). *J. Volc. Geotherm. Res.*, 102, 21–44.

37. Wandji, P.,Wotchoko, P., Bardintzeff, J-M., &Bellon, H. (2010). Late Tertiary and Quaternary alkaline volcanism in the westernNoun Plain (Cameroon Volcanic Line): New K-Ar ages, petrologyand isotope data. *Geochemistry, Mineralogy and Petrology*, 48, 67-94.

38. Wang, K., Plank, T., Walker, J.D., & Smith, E.I.(2002). A mantle melting profile across the Basin and Range, SW USA. *Journal of Geophysical Research* 107,

39. Mbassa, B.J., Njonfang, E., Benoit, M., Kamgang, P., Gregoire, M., Duchene, S., Brunet, P., Ateba, B., and Tchoua, F. M. (2012). Mineralogy, geochemistry and petrogenesis of the recent magmatic formations from Mbengwi, a continental sector of the Cameroon volcanic line (CVL), Central Africa. *Mineral.Petrol.*, 106, 217–242.

40. Pearce, J. A. (2014). « Immobile element fingerprinting of ophiolites. » Elements 10(2), 101-108.

41. Shervais, J. W. (1982). « Ti-V plots and the petrogenesis of modern and ophiolitic lavas. » *Earth and Planetary Science Letters* 59(1): 101-118.

42. Condie, K. C. (2005). « High field strength element ratios in Archean basalts: a window to evolving sources of mantle plumes? » *Lithos*79(3-4): 491-504.

43. McKenzie, D., &O'Nions, R.K. (1991).Partialmelt distributions from inversion of rare earth element concentrations. *J Petrol* 32:1021–1091.

44. McDade, P., Blundy, J.D, &Wood, B.J. (2003). Trace element partitioning on the Tinaquillo Lherzolite solidus at 1.5 GPa. *Phys Earth Planet Inter* 139:129–147.

45. Yokoyama, T., Aka, F.T., Kusakabe, M., and Nakamura, E. (2007). Plume-lithosphere interaction beneath Mt. Cameroon volcano, West Africa: Constraints from 238U-230Th-226Ra and Sr–Nd–Pb isotope systematic. *Geochim. Cosmochim. Acta*, 71, 1835–1854.

394

395

396

397